2008 IEEE International Conference on
Robotics and Automation
Pasadena, CA, USA, May 19-23, 2008

The Influence of DC Electric Drives on Sizing Quadruped Robots

Panagiotis Chatzakos, and Evangelos Papadopoulos, *Senior Member, IEEE*

Abstract— **In legged systems design an important question applies to: "What can be inferred from the performance of a legged robot of a similarly configured system, but scaled to a smaller or larger size?" Our work attempts to answer this question and set the basis for a systematic approach in sizing legged robots. This paper focuses on the influence of permanent magnet DC electric drives on the size of quadruped running robots. The reason is twofold. First, many of the existing legged machines have used such actuators for propulsion. The second, the performance of electric motors scales differently from torque-speed requirements of legged robots. Specifically, we show that there exists a particularly sized quadruped running robot that is superior according to desired performance criteria, and under the existing technologic limitations and economic restraints. Therefore, valuable information on legged systems design and insight for optimizing the size of a quadruped robot emerges.**

I. Introduction

It is generally accepted that the performance of different subsystems may scale differently. This is very important in complex systems, such as legged robots. For example, actuator performance typically scales in a completely different way to structural strength, [1]. Analysis of the ways in which different subsystems scale, permits conclusions to be drawn about the necessity for configuration changes, i.e. changes in the type of actuator, or in the structural material.

Nondimensional numbers that combine important system parameters are particularly useful when dealing with systems that have similar configuration but different scale. We are all familiar with the role of the Reynolds number in fluid mechanics as an indicator of the onset of turbulence, [2]. Similarity analysis and its role in experimental mechanics is also well established in engineering practice.

A relevant example of a scaling law is provided by the Froude number, [3]. The Froude number is twice the ratio of the kinetic energy to the gravitational potential energy of a system. Particularly in legged locomotion, the Froude number has been shown to be a predictor of dynamic gait transitions in animals of widely differing size. That is, animals will tend to transition from a walk to a trot, and from a trot to a gallop at similar values of the Froude number, [4].

This work is co-funded by public (European Social Fund 75% and General Secretariat for Research and Technology 25%) and private funds (Zenon SA), within measure 8.3 of Op. Pr. Comp., 3rd CSP-PENED'03.

Panagiotis Chatzakos is with the Department of Mechanical Engineering, National Technical University of Athens, Greece (phone: +30-697-746-7158; e-mail: pchatzak@mail.ntua.gr).

Evangelos Papadopoulos is with the Department of Mechanical Engineering, National Technical University of Athens, Greece (phone: +30-210-772-1440; fax: +30-210-772-1450; e-mail: egpapado@central.ntua.gr).

In small-scale, electric power is the predominant source of energy. Small-scale electric power supplies (batteries), actuators, controls and sensors are common and well developed. To date, many of the legged machines produced have used electromagnetic motors for propulsion, e.g., [5], [6], [7], and [8]. Although there are many tools to help the designer to choose the right motor drive for a particular application, a systematic methodology or a dedicated tool that connects the size of the motor-gearbox combination with the size of the robot does not exist. In this paper, we are setting the basis of a methodology to assist the designer to choose the optimal size of the robot according to some specification, given the constraints that existing electric drives impose.

Initially, simple scaling laws are derived from first principles where the basis for these laws is obvious. The techniques for developing electric scaling laws are discussed comprehensively. The developed electrical scaling laws examine resistive, magnetic, and electrostatic effects, as in [9], and they are verified by using data from existing systems. Combining the simple scaling laws with each other, and with engineering relationships, produces more complex and less intuitive laws. Applications of the scaling laws are then used to provide direction in optimal quadruped robot design.

Connecting the size of the motor drive with the size of the legged machine departs from that in [10], where scaling concepts for running robots are discussed and a parametric analysis for a quadruped, passively bounding, robot is presented. According to that analysis, dynamically similar motions may be obtained for a wide range of dimensionless parameters related to the "shape" of the legged machine. Broadly speaking, "shape" refers to the analogies between the structural components of the robot, such as body and leg length, body mass and inertia, leg stiffness, and hip separation.

It was shown that energy consumption varies for different combinations of structural parameters, and that these differences are considerable, [10]. Consequently, to minimize energy expenditure one should identify the set of parameters, for which the required energy to sustain the desired motion is the least. Although the result of this process is the optimal shape of the running quadruped, i.e. the optimal analogies between its structural components, yet it reveals nothing about the optimal size of the legged robot.

This information is obtained through the work provided here. In this paper, we show that there exists a particular size of the quadruped running robot that is superior according to desired performance criteria, which are in turn subject to the existing technologic limitations and market economic re-

Authorized licensed use limited to: Technische Universitaet Muenchen. Downloaded on December 11,2021 at 13:19:11 UTC from IEEE Xplore. Restrictions apply.

straints. This result provides valuable insight into legged machine design and sets the basis of a methodology to assist the designer to choose the optimal size of the robot according to some specification.

II. Similarity Rules

A similarity rule maintains the constancy of a nondimensional number. The simplest similarity rule is geometric similarity. Here, the ratio of any lineal dimension to a characteristic length of the system is constant. That is, all dimensions are magnified by the same factor as compared to a base configuration. For example, if the same materials are used, the mass of a system scales with the cube of the length in geometrically similar systems.

Just as geometric similarity refers to shapes, the concept of dynamic similarity refers to motion. Two motions are said to be dynamically similar if one could be made identical to the other by multiplying all linear dimensions by some constant factor and all time intervals by another one. Additionally, dynamic similarity in legged locomotion requires that the Froude numbers of the motions of two legged animals (or robots) are equal.

According to the parametric analysis in [10], the rest of the dimensionless parameters that should be kept equal for dynamically similar motions are the combinations of the structural parameters, which are connected to robot shape as discussed in Section I. Particularly, these combinations of the design parameters include: (a) the dimensionless inertia *j*, i.e. the robot's body inertia, normalized to the product of body mass and the square of hip separation, (b) the leg relative stiffness *r*, which is defined as the product of leg stiffness and leg rest length normalized to the weight of the robot, and (c) the ratio of hip separation to the height of center of mass (or the leg rest length), given as *p*.

Next, we use an evidential example based on biological data to prove similarity requirements. Let the rest leg length be the characteristic scale length. This implies that by doubling the rest length of the leg, the robot is scaled up by a factor of two. Body mass is proportional to the third power of the characteristic length while the gravitational acceleration does not scale with size. Therefore, in order for the robot to keep moving in a dynamically similar fashion, the leg stiffness should be quadruplicated, since the relative stiffness of the leg should be kept constant. This is consistent with biology findings in animal scaling laws, [11], where the leg springiness increase with body mass, namely, $k \propto m^{2/3}$.

III. Scaling Laws

The techniques for developing scaling laws for electromagnetic subsystems are derived and explained here. Specific scaling laws are developed and verified using data from existing systems. Finally, applications of the scaling laws are discussed to help provide direction in quadruped robots design.

The laws developed provide the variation of the property of interest with respect to the scale factor, i.e., the characteristic length. Another size scale factor, such as the product of the characteristic length and system weight, could be used as well and, while the individual scaling laws would be different, the relationships between scaling laws would be invariant.

Initially, simple scaling laws are derived from first principles where the basis for these laws is obvious. More complex and less intuitive laws may be produced by combining these simple scaling laws with each other and with engineering relationships. Laws are expressed as an exponent of the characteristic length. All scaling laws presented here are, by their nature, simplistic and applicability over a wide range may be limited. It is important to remember that these laws are intended to provide guidance and intuition into the domain but are not meant as a substitute for detailed analysis.

A. Electric motors

Most macroscopic electric motors rely on magnetic fields produced by electric currents or permanent magnets. As shown in Table I, where the electric motor scaling laws are summarized, the magnetic field produced by magnets is invariant with scale.

TABLE I
Electric Motor Scale Laws

Name	Formula	Order	Variables
Area	$A \propto l^2$	2	l - Characteristic length (1)
Mass	$M \propto (\rho, l^3)$	3	ρ - Material density (0)
Armature resistance	$R_a = \frac{1}{c_w}\frac{l_w}{\pi r_w^2}$	-1	c_w - Wire conductivity (0) l_w - Wire total length (1) r_w - Wire diameter (1)
Magnetic force on (still) conductor	$F = Bl_r\frac{V_a}{R_a}$	2	B - Magnetic field (0) l_r - Rotor length (1) V_a - Armature voltage (0)
Motor (stall) torque	$\tau_m = N_c B l_r \frac{V_a}{R_a} r_r$	4	r_r - Rotor radius (1) N_c - Number of conductors (1)
Stress-induced speed limit	$\omega = \frac{1}{r}\sqrt{\frac{8\sigma}{(3+\nu)\rho}}$	-1	ν - Poisson's ratio (0) σ - Allowable stress (0) r - Disk radius (1)
Gearing load factor	$K_v = \frac{C}{C + V_m^{0.5}}$	-0.5	V_m - Pitch-line speed (1) C - Constant (0)
Motor scale length	$s_m = \sqrt[3]{\pi r_m^2 l_m}$	1	r_m - Motor radius (1) l_m - Motor length (1)

In an electric motor the magnetic force on a moving conductor frequently provides the forced to operate the motor. The force on a still, current carrying, conductor is a second order law. Motor stall torque is the product of that force acting on multiple conductors that increase in number with scale, and rotor radius and thus it is a fourth order law.

Empirical evidence for these scaling laws is easily found. For example, consider the fourth order torque scaling law.

Authorized licensed use limited to: Technische Universitaet Muenchen. Downloaded on December 11,2021 at 13:19:11 UTC from IEEE Xplore. Restrictions apply.

Fig. 1 is the plot of motor size vs. stall torque for a series of commercially available permanent magnet DC motors, [12]. The motor scale length here is defined as the cube root of the motor volume (see Table I). The correlation between "actual" and "prediction" values using the fourth order scaling law is very strong.

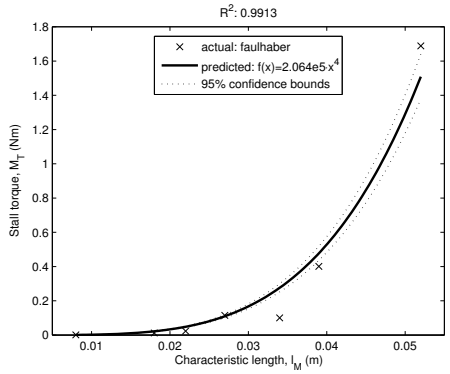

Fig. 1. Motor size vs. stall torque for a series of commercially available permanent magnet DC motors ([12]).

B. Planetary gearheads

In most instances, electric motors run at far higher speeds than are suitable for quadruped robot joints and therefore gearboxes are used to match motor speed to joint speed. Space, and the diverse configurations and mechanics of gearboxes that are actually used, preclude a detailed discussion of the scaling of gearboxes here, especially of the planetary ones that are mostly used in legged robots. However, since speed is inversely proportional to motor size as indicated in Table I, scaling down can result in very high motor speeds requiring large speed reduction ratios.

The transmitted load through the gearbox depends heavily on the accuracy of the gears. A dynamic load factor is added by manufacturers to take care of this. For gears of the precision classes, the strength of the gear tooth depends, among others, on the square root of surface speed, which is often also referred to as pitch-line speed. Therefore, the load factor is an inverse square root order law of motor size (see Table I). This is also empirically evident. Fig. 2 displays motor size vs. maximum permissible speed for a series of commercially available precision planetary gearheads ([12]).

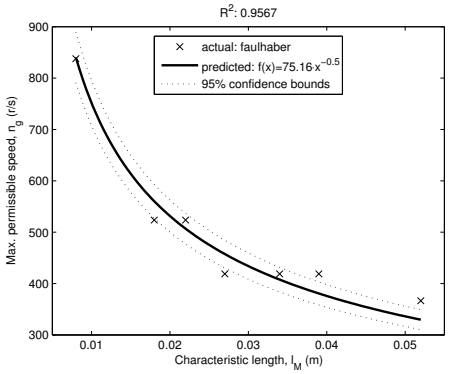

Fig. 2. Motor size vs. max. permissible speed for a series of commercially available precision planetary gearheads ([12]).

Practical reduction ratio achievable any type of planetary gearheads is limited. Furthermore, high ratios mean multiple reduction stages. The number of stages of speed reduction is a concern not only because of the relative bulk, weight and complexity of multi-stage reducers, but also because efficiency degrades exponentially with the number of reduction stages.

IV. System Dynamics

Fig. 3 shows a planar model that is used to study the influence of permanent magnet DC motors on the size of quadruped robots. This is a commonly used template to analyze the basic qualitative properties of quadrupedal running. Its associated parameters are given in Table II.

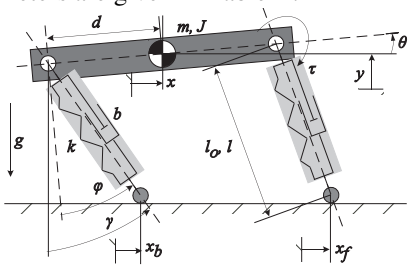

Fig. 3. Parameters of the template for quadrupedal bounding in plane.

TABLE II
VARIABLES AND INDICES USED

x	COM horizontal pos.	τ	torque delivered at hip
y	COM vertical pos.	g	acceleration of gravity
θ	body pitch angle	m	body mass
γ	leg absolute angle	J	body inertia
φ	leg relative angle	d	hip joint to COM distance
x_{bt}	back toe horizontal pos.	f	as index: front leg
x_{ft}	front toe horizontal pos.	b	as index: back leg
l	leg length	m	as index: motor
l_o	leg rest length	$*$	as subscript: dimensionless

This model, which represents the lateral half of a quadruped, and consists of a rigid body and two springy massless legs, one attached to the body at the front and the other attached at the rear. Permanent magnet DC electric motors control the orientation of each leg with respect to the body and the torque delivered to each leg. Each modeled leg represents the back or the front leg pair, in which the two back or front legs are always in phase, and it is called virtual leg, [6]. Each virtual leg has twice the stiffness of a single leg. The torque delivered at the hip of each robot leg is equal to half the corresponding ones at the virtual leg.

Based on the fact that simplified models, and passive dynamics, have been already proved to be helpful in designing controllers, [6], we use an unactuated and conservative model, which encodes the target behavior of the system and reveals intrinsic system properties and aspects of quadrupedal bounding, and it is anticipated to be used as a testbed for the validation of the discussed concept.

To reveal the effect of scaling, dimensional analysis is employed and a passive and conservative model is derived using a Lagrangian formulation, with generalized coordinates the Cartesian variables describing the center of mass COM position and the main body's attitude. The detailed model is

Authorized licensed use limited to: Technische Universitaet Muenchen. Downloaded on December 11,2021 at 13:19:11 UTC from IEEE Xplore. Restrictions apply.

described in [10] thoroughly, yet is given here as a set of differential-algebraic equations to complement the analysis

$$\dot{x}^* = -r\left(1-l_b^*\right)\sin\left(\theta^*+\phi_b^*\right) - r\left(1-l_f^*\right)\sin\left(\theta^*+\phi_f^*\right) \quad (1)$$

$$\dot{y}^* = r\left(1-l_b^*\right)\cos\left(\theta^*+\phi_b^*\right) + r\left(1-l_f^*\right)\cos\left(\theta^*+\phi_f^*\right) - 1 \quad (2)$$

$$\dot{\theta} = r\left(\left(1-l_f^*\right)\cos\phi_f^* - \left(1-l_b^*\right)\cos\phi_b^*\right)\Big/ p\ j \quad (3)$$

$$\begin{aligned}\phi_b^* &= \text{Atan2}\left(y^* - p\sin\theta^*, x_{bt}^* + p\cos\theta^* - x^*\right) - \theta^* \\ \phi_f^* &= \text{Atan2}\left(y^* + p\sin\theta^*, x_{ft}^* - p\cos\theta^* - x^*\right) - \theta^*\end{aligned} \quad (4)$$

$$\begin{aligned}l_b^* &= \sqrt{\left(x_{bt}^* - x^* + p\cos\theta^*\right)^2 + \left(p\sin\theta^* - y^*\right)^2} \\ l_f^* &= \sqrt{\left(x_{ft}^* - x^* - p\cos\theta^*\right)^2 + \left(p\sin\theta^* + y^*\right)^2}\end{aligned} \quad (5)$$

In order to facilitate the study, we focus on system periodic steady state trajectories, which are trajectories that repeat themselves after one cycle of locomotion. Following a similar procedure as in and [6] and [10] we employ a Poincaré Map technique to formulate these trajectories.

V. Motor Effect Study

Following the previous assumptions, the robot executes a passive motion according to the sets of initial conditions, found by employing the Poincaré Map technique, which is in favor of its natural dynamics. In this case, no energy is lost or added to the system. This may sound unrealistic, but if one uses actuators just to compensate for the lost energy, and initial conditions that yield a passive trajectory, then the robot will execute an active gait, very close to the passive gait and the system can be then studied as in the lossless case, which is described by (1)-(5).

The only energy required then to sustain the motion is the amount dissipated over one stride, which is the sum of the mechanical energy dissipated due to leg friction and the kinetic energy lost in ground damping and compression at touchdown. This amount of energy is injected into the system by the motors, which are controlled to exert a desired constant torque that is given, in its dimensionlesss form, as

$$\tau^* = \tau/\left(m\,g\,l_o\right) \quad (6)$$

The dimensionless angular velocity about a joint, is given as

$$\omega^* = \omega\sqrt{l_o/g} \quad (7)$$

Generally speaking, in work cycles, all operating points must lie beneath the motor curve at a maximum voltage. Mathematically, this means that the following must apply for all operating points (ω,τ)

$$1 > \frac{\omega}{\omega_o} + \frac{\tau}{\tau_{stall}} \quad (8)$$

where ω_o is the no-load speed, and τ_{stall} is the stall torque. Apparently, the performance of the electric drive is limited by other factors, as well, from which the prime are the maximum permissible speed at gearbox input and the maximum permissible continuous torque delivered due to thermal considerations.

According to the analysis presented in Section III, motor stall torque and no-load speed in (8) can be scaled as

$$\tau_{stall} = \tau_{stall}^* m_m g\, s_m \quad (9)$$

$$\omega_o = \omega_o^*\sqrt{g/s_m} \quad (10)$$

since motor mass scales with the cubic power. (Refer to Tables II and III for the associated indices and variables.)

By substituting (6) to (10) in (8), a nondimensional form of the motor-load curve, i.e. a universal motor-load curve, results as

$$1 > \frac{l_o^{-0.5}\, i_g \omega^*}{l_m^{-0.5}\,\omega_o^*} + \frac{m l_o\, \tau^*}{m_m\, s_m\, \tau_{stall}^*\, i_g\, n_g} \quad (11)$$

where i_g is the reduction ratio and n_g is gearbox efficiency. This universal motor-load curve drawn here refers solely to the electric drives selected for this study. However, the methodology for constructing such a curve is not restricted to these but could apply to all electrically driven systems, or could be derived from data from different motor vendors.

Nowthen, in nondimensional work cycles, all operating points must lie beneath the universal curve at a maximum voltage. The scaling factors of the motor, based on which the universal curve is drawn, depend on the existing range of commercially available permanent magnet DC motors from [12]. Their range of products is finite due to technology limitations and economic restraints, i.e. in larger scale, it is much more cost effective to use other electric actuation technologies and in micro-scale systems, motors operating on other than electromagnetic principles are needed. For the purpose of the work here we use the scaling factors presented in Table III, which are derived from scaling the smoovy DC Drives from [12] based on the analysis presented in Section III.

TABLE III
SMOOVY DC DRIVES SCALING FACTORS

Description ($= f$)	Factor ($= C$)	Value	Function
Max. motor speed vs. scale ($= s$)	$\omega_{\max}^*$	112.6	$f(s) = C \cdot s^{-1}$
No-load speed vs. scale	ω_o^*	316.9	$f(s) = C \cdot s^{-1/2}$
Max. permissible speed vs. scale	ω_g^*	75.2	$f(s) = C \cdot s^{-1/2}$
Stall torque vs. size ($= m\,g\,s$)	τ_{stall}^*	33.0	$f(x) = C \cdot x^1$
Max. permissible torque vs. scale	$\tau_{\max}^*$	5.3	$f(s) = C \cdot s^4$
Motor equivalent density vs. scale	ρ_m	5282.0	$f(s) = C \cdot s^0$
Reduction vs. No. of stages ($= N$)	C_1	1.4	$f(N) = 1 \cdot e^{C \cdot N}$
Efficiency vs. No. of stages (%)	C_2	0.1	$f(N) = 100 \cdot e^{-C \cdot N}$

The ratio of leg length to motor characteristic length and the ratio of robot mass to motor mass that appear in (11) reflect the analogy between the sizes of the robot and the motor(s). In that sense, by comparing the length or mass ratios of various robots for a given motor size, a larger length ratio means that the size of the robot is relatively larger, and a larger mass ratio means that the robot is capable of carrying bigger payload, if the structural mass is kept constant. Likewise, for given robot size, a larger mass ratio implies

Authorized licensed use limited to: Technische Universitaet Muenchen. Downloaded on December 11,2021 at 13:19:11 UTC from IEEE Xplore. Restrictions apply.

that the size of the actuator needed to propel the robot and the desired payload is relatively smaller.

In Fig. 4, the universal motor curve along with various load curves, drawn by simulation of the passively stable bounding quadruped described by (1)-(5), for increasing length (upper) and mass (lower) ratios are presented. Dimensionless forward speed, which is defined as

$$v^* = \dot{x} \Big/ \sqrt{g\, l_o} \tag{12}$$

varies from 0.9 to 3.0, which corresponds to typical bounding speeds found in nature. The rest of the dimensionless design parameters are kept constant. Each marker on the load curves corresponds to the maximum required speed and torque in a passive bounding cycle with zero pitch rate (i.e. pronking), while the background color of the marker corresponds to the value of the dimensionless forward speed.

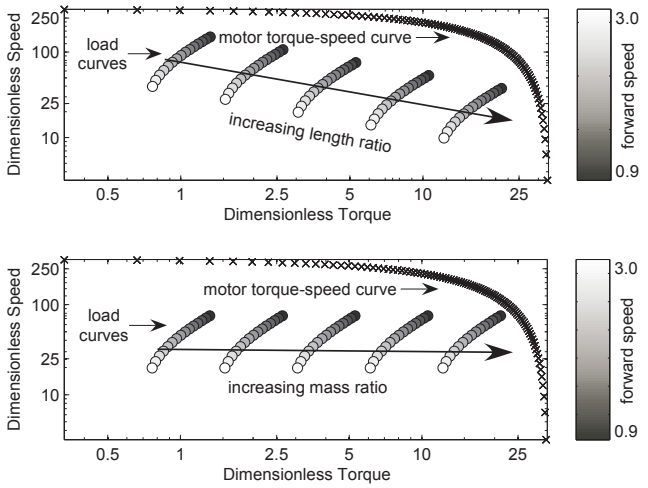

Fig. 4. The universal motor curve and dimensionless load curves for various combinations of length (upper) and mass ratio (lower).

Since the mass of a system is typically scaled up with the third order law of the characteristic length, the separate length and mass ratios could be reduced to a single ratio using the corresponding densities, namely motor and robot equivalent densities. Motor equivalent density is derived from motor data (see Table III), while robot equivalent density is estimated by a series of biological data extracted from various experimental biology publications. Fig. 5 presents the leg length, which is the typical scale factor for living and artificial quadrupeds, versus body mass for a series of quadruped animals, from small rats to large horses.

We assign the estimated equivalent density to robot density because one may fairly consider that nature's designs are optimized even though animal requirements are way different than those of machines. Such a choice is not misleading, since a different choice may affect the actual results but not the essence of the proposed methodology. To support this, we add data from existing robots in Fig. 5, namely for Scout-II, RHex and Tekken, which they satisfactorily fit the third order scaling law ([5], [6] and [7]). Therefore, the estimated equivalent robot density is found to be 218.6, and it will be used next.

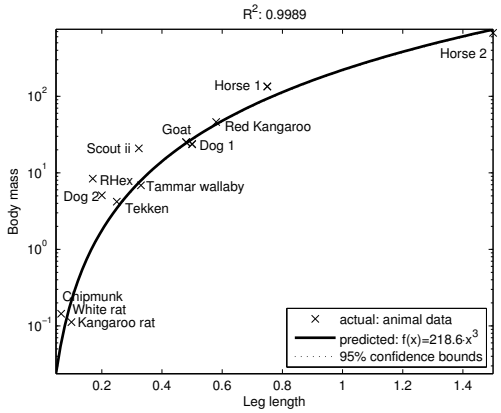

Fig. 5. Leg length vs. body mass for a series of quadruped animals.

The minimum value of the mass ratio can be obtained by taking into account that an actuated quadruped robot should have at least four motors. If the mass of the planetary gearboxes is fairly added, then reasonable robot to motor mass ratios should be way over 12 based on Fig. 6, where the unit mass increase versus the reduction ratio for a series of commercially available precision planetary gearheads ([12]). We consider a minimum mass ratio of 12 and therefore the minimum length ratio results as

$$\frac{m}{m_m} \geq 4(1+2) \Rightarrow \frac{\rho l_o^3}{\rho_m l_m^3} \geq 12 \Rightarrow \left.\frac{l_o}{s_m}\right|_{\min} = \sqrt[3]{12\frac{\rho_m}{\rho}} \tag{13}$$

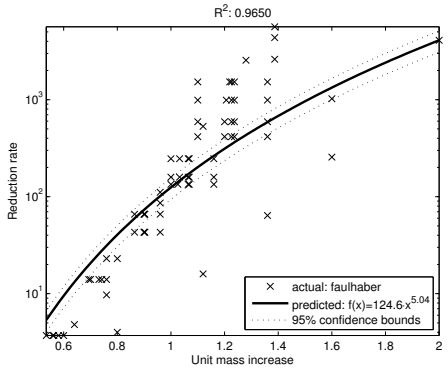

Fig. 6. Unit mass increase vs. reduction ratio for a series of commercially available precision planetary gearheads ([12]).

The maximum permissible speed of the motor is limited by the maximum input speed at gearbox. Given the minimum length ratio as in Eq. (13), and forcing the operating speed to be less than the maximum permissible, which scales according to Table III, then a maximum reduction ratio can be obtained as

$$\sqrt{\frac{1}{l_o}} i_g\, \omega^* \leq \sqrt{\frac{1}{s_m}}\, \omega_g^* \Rightarrow \left. i_g \right|_{\max} = \frac{\omega_g^*}{\omega^*} \sqrt{\frac{l_o}{s_m}} \tag{14}$$

An electric motor will rarely deliver its stall torque due to thermal considerations. Its maximum continuous operating torque is limited by environmental factors and the amount of heat that can dissipate. Therefore, the maximum required torque should be kept below the maximum permissible motor torque, which is scaled according to Table III. This assump-

Authorized licensed use limited to: Technische Universitaet Muenchen. Downloaded on December 11,2021 at 13:19:11 UTC from IEEE Xplore. Restrictions apply.

tion leads to the maximum mass ratio as

$$\frac{m l_o \tau^*}{i_g n_g} \le m_m s_m \tau^*_{\max} \Rightarrow \left.\frac{m}{m_m}\right|_{\max} = \frac{i_g n_g \tau^*_{\max}}{\tau^*} \left(\frac{l_o}{s_m}\right)^{-1} \quad (15)$$

VI. Results

Following the methodology presented in Section IV, we seek here the optimal mass ratio for a quadruped robot of total mass m = 15 kg, 5 kg of which is the largest allowable payload m^p. The desired dimensionless forward speed number ranges between 0.9 and 3.0. By using (13) and the estimated values for the equivalent densities of both the motor and the robot from Table III and Fig. 5, respectively, the minimum length ratio is found to be 6.8. The dimensionless torque and angular speed, given by (6) and (7), respectively, are calculated as in Fig. 4. The dimensionless angular speed, the computed minimum leg length, the scale constant ω_g^* of the maximum permissible speed at gearbox input and (14) are combined to obtain the maximum allowable reduction rate. Finally, the dimensionless torque, the minimum leg length, the maximum reduction rate, gearbox efficiency, which is derived from Table III in two steps, and (15) are used to obtain the optimal mass ratio, which is plotted in Fig. 7 (A) versus the dimensionless forward speed.

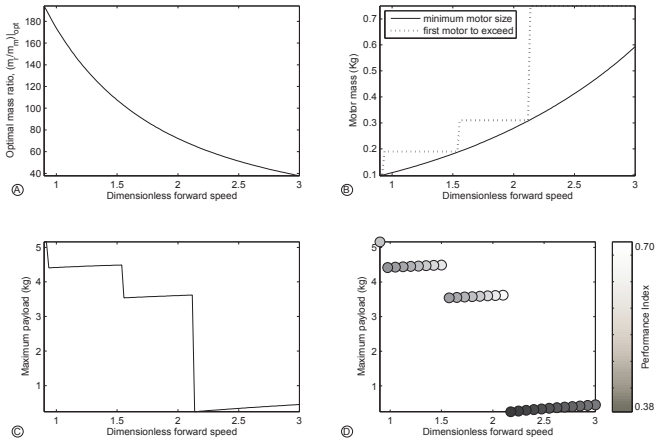

Fig. 7. Opt. mass ratio (A), min. motor mass and the first motor that exceeds (B), the max. payload (C) and P.I. (D) vs. the dimensionless speed.

By dividing the optimal mass ratio with the overall robot total mass the minimum motor mass is obtained, and it is drawn in Fig. 7 (B). Considering the actual motor masses and the fact that there is not an infinite number of winding variations available from a practical point of view, this line should be replaced by the discontinuous dotted line, which represents the first available motor to exceed the minimum required motor mass. This is illustrated in Fig. 7 (B), as well.

There appears to be a tradeoff between the maximum achievable speed and the maximum payload that a robot may carry if actuated with a certain motor. Moving with greater speed necessitates bigger motors and result to less payload, if the total mass is kept constant. This is evident in Fig. 7 (C). Exactly at the point where the step change for a bigger motor is introduced the capability of a particular motor is fully exploited. This constitutes an optimal selection by itself.

By further defining a performance index, such as the weighted sum of relative payload, i.e., divided by the maximum required, and relative forward speed, i.e., divided by the maximum possible,

$$\text{P.I.} = w_m \frac{\mathrm{m_i^p}}{\max\left(\mathrm{m_i^p}\right)} + w_v \frac{v_i^*}{\max\left(v_i^*\right)} \quad (16)$$

one could identify that combination of payload and forward speed, for which the P.I. in (16), is least, and thus obtain the optimal size of the robot. In Fig. 7 (D) the value of the P.I. for the case of an equally weighted sum, i.e., for $w_m = w_x = 0.5$, is drawn. P.I. is maximized for a payload of 3.6 kg and a dimensionless forward speed of 2.1. Ultimately, a 0.31 kg motor should be selected for this particular robot.

Conclusion

In this paper, electric scaling laws were developed and verified by using data from existing systems. Applications of the scaling laws were discussed for the case of a bounding quadruped robot executing an active gait very close to the passive one. The critical issue of how big the robot should be was explored. The work was focused on the influence of permanent magnet DC electric drives on the size of the robot and it has been showed that there exists a particularly sized quadruped that is superior according to given specification. This constitutes a useful guideline in design quadruped robots and facilitates optimal legged machine design.

References

[1] Waldron, K.J. and Hubert, C., "Scaling of robotic mechanisms", *Proc. of the 2000 IEEE Int. Conf. on Robotics & Automation*, Vol. 1, 2000, pp. 40-45.

[2] Reynolds, O., "An experimental investigation of the circumstances which determine whether the motion of water shall be direct or sinuous, and of the law of resistance in parallel channels", *Philosophical Trans. of the Royal Society*, 174, 1883, pp. 935-982.

[3] "Froude number", in *Encyclopædia Britannica*. From Encyclopædia Britannica Online: http://www.britannica.com/eb/article-9035514.

[4] Alexander, R. McN., "Terrestrial Locomotion", *Mechanics and Energetics of Animal 1ocomotion*, eds. Alexander R. McN. and Goldspink, G., Chapman and Hall, London, 1977.

[5] Saranli U., Buehler M., and Koditschek D.E., "RHex: A Simple and Highly Mobile Hexapod Robot", *International Journal of Robotics Research*, Vol. 20, No. 7, 2001, pp. 616-631.

[6] Poulakakis I., Papadopoulos E. G. And Buehler M., "On the Stability of the Passive Dynamics of Quadrupedal Running with a Bounding Gait", *Int. J. of Robotics Research*, Vol. 25, 2006.

[7] Kimura H., Fukuoka Y. and Cohen H., "Adaptive Dynamic Walking of a Quadruped Robot on Natural Ground based on Biological Concepts", *Int. J. of Robotics Research*, Vol.26, No.5, 2007, pp.475-490.

[8] Nichol J. G., Singh S. P.N., Waldron K. J., Palmer L. R. III, and Orin D. E., "System Design of a Quadrupedal Galloping Machine", *Int. J. of Robotics Research*. Vol. 23, No10-11, 2003, pp. 1013-1027.

[9] Spletzer Barry, "Scaling Laws for Mesoscale and Microscale Systems", *IEEE Trans. on CPMT - Advanced Packaging*, 1999.

[10] Chatzakos P. and Papadopoulos E. G., "Parametric Analysis and Design Guidelines for a Quadruped Bounding Robot", *Proc. of the 15th Mediterranean Conf. on Control and Automation*, 2007, Greece.

[11] Farley C.T., Glasheen J., and McMahon T.A., "Running Springs: Speed and Animal Size", *J. of Experimental Biology*, Vol. 185, 1993.

[12] www.faulhaber-group.com, smoovy® Miniature Drive Systems.

Authorized licensed use limited to: Technische Universitaet Muenchen. Downloaded on December 11,2021 at 13:19:11 UTC from IEEE Xplore. Restrictions apply.